RESEARCH PAPER

ALTITUDINAL APPRAISAL OF LAND USE LAND COVER AND SURFACE TEMPERATURE CHANGE IN THE SATLUJ BASIN, INDIA

Pankaj Kumar[1], Swati Thakur[2*], Surajmal Junawa[1], Subhash Anand[1]
[1]Department of Geography, Delhi School of Economics, University of Delhi, Delhi, India
[2]Department of Geography, Dyal Singh College, University of Delhi, New Delhi
***Corresponding author:** swatithakur.dsc@gmail.com
Received: July 29th, 2023 / Accepted: November 14th, 2023 / Published: December 31st, 2023
https://DOI-10.24057/2071-9388-2023-2958

ABSTRACT. The land use change has affected nearly 32% of the global landscape from 1960 to 2019. Several studies have examined the impacts of land use land cover (LULC) on the surface temperature. Still, the spatiotemporal variation of LULC and LST with altitude is a less researched area. In the current study, we assess the LULC dynamics and its relation to altitudinal LST in the Himalayan Satluj River basin in Himachal Pradesh across the altitudinal range of 332 to 6558 meters. LULC, LST, NDVI, and NDMI were derived from Landsat data for 1980-2020. The spatial pattern was analyzed using Support Vector Machine (SVM) and a mono-window algorithm. The results of LULC denote that snow covered area (SCA) have decreased by nearly 56.19% since 1980 and vegetation cover has increased. However, a decline in vegetation density is pronounced at the same time. The mean surface temperature of the Satluj basin has amplified by 6°C (0.25°C/year) from 1996 to 2020. Mostly Zone 3 and 4 are under high hilly and temperate dry regions in Lahaul Spiti and Kinnaur district of Himachal Pradesh. The most important sign is that the mean surface temperature for Zone 3 (3000m-4500m) and Zone 4 (above 4500m) was the highest increase to 6°C (0.26°C/year) and 8°C (0.31°C/year) from 1996 to 2020. The increase in LST values is attributed to land cover dynamics precisely the decline of snow cover area and the emergence of vegetation zone at higher above the 4500 altitudes. Our study facilitates regional analysis.

KEYWORDS: Land use land cover; Land surface temperature; Altitudinal Variation; Satluj Basin; Climate changes

CITATION: Pankaj Kumar, Swati Thakur, Surajmal Junawa, Subhash Anand (2023). Altitudinal Appraisal Of Land Use Land Cover And Surface Temperature Change In The Satluj Basin, India. Geography, Environment, Sustainability, 4(16), 26-38
https://DOI-10.24057/2071-9388-2023-2958

Conflict of interests: The authors reported no potential conflict of interest.

INTRODUCTION

Among geographical regions mountains are the most sensitive to climate changes (Xystrakis et al. 2017). Witnessing some of the clearest evidences such as melting of glaciers, rise of temperature and increasing intensity of extreme events (Bandyopadhyay et al. 2023), mountains not only are at risk but they affect the adjacent lowland population and environment too. Moreover, the implications are likely to be faced by entire geosystem (Lutz et al., 2013) due to inter regional linkages involving mass and energy exchange. One of the prime drivers affecting mountain ecosystem is the pressure of land use and land cover (LULC) change leading to compromises in its capacity to provide its ecosystem services (Husain et al. 2023; John et al. 2022; Pang et al. 2022). Mountains being home to 15 per cent of world's population the changing climate and demography are bound to have environmental and societal consequences transversely elevations. Land transformations are mainly altered by anthropogenic pressure to maximize the economic benefits of human. The main drivers of the land transformations and global climate are amplified by the urbanization, over population, expansion of settlement, construction of roads, deforestation, changing agriculture pattern, exploitation of natural resources, tourism, demand of energy especially hydro projects in mountain regions (Chauhan et al., 2021; Chhogyel et al., 2020; Roy et al., 2022; Upadhayaya, 2015). Global climate change and increasing anthropogenic pressure are affecting regional biodiversity ecosystem and sustainable development. Climate change, and increasing intensity and frequency of natural events have effects on SDGs such as SDG 1 (no poverty), SDG 3 (good health and wellbeing), SDG 11(sustainable communities) SDG 13 (Climate action), and availability & accessibility of resources.

Himalayan mountain geosystem provides millions of lowland and downstream populations with life sustaining vital nutrients such as water and soil. The changes in land utilization pattern (land use) viz. deforestation and intensification of agricultural areas by humans and biophysical cover of surfaces (land cover) are dominant transitions which have impacted the historiography of landscape patterns. The worry is that the recent transitions coupled with natural climatic changes have challenged the long term ecosystem services (Young, 2014). Detailed multi temporal change studies will provide better understanding of the challenges posed due to changes in landscape making regional sustainability complex as people's livelihoods depend on natural resources in mountain areas. Land Surface Temperature (LST) provides useful information regarding water, heat and land surface processes (Bindajam et al. 2020). It is one of the most effective factors for understanding the regional climate, surface energy balance, vegetation change in the highland-lowland regions (Holzman et al. 2014; Taripanah et al. 2021). The evaluation of LST hence is another significant factor pertinent to environmental change studies.

The whole Himalayas doesn't respond the same to alterations of the landscape and character of surface temperature and encompass variation at the regional level (Rani et al. 2022). It is affected by changes in many ways such as degradation of land, increasing climatic variability, landslide hazards, depletion of groundwater, soil erosion, etc. (Ali et al. 2019; Grêt-Regamey et al. 2014; Swain et al. 2022; Vannier et al. 2019; Wen et al. 2020). The spatial temporal distribution of energy exchange is also affected by topographical, metrological, vegetation and soil character shaping the geophysical setting (Li et al. 2015).

Among the different river basins which connect the highland lowland interactive systems, the Satluj basin comprises a landscape with distinct climatic condition, elevation gradient, intense agriculture matrix, expanding hydro power and urban centres in lowland area, all posing pressure to native ecosystem and its services. It is not far from these changes, the rising surface temperatures at the river's higher altitudes make sustainability difficult at local level.

The analysis of landuse land cover dynamics from available public domain data by elevation and geographic setting and to integrate with changes in land surface temperature characteristics would be first step to the study of its ecosystem service dynamics and challenges to its sustainability. Within this context our study presents the first element of this framework and specifically addresses two research objectives: i) to analyse LULC and Land Surface Temperature (LST) change pattern across biophysical and altitudinal settings of Sutlej basin in terms of rate, magnitude and direction of change, ii) to contextualise the environmental and anthropogenic driving factors to explain the transition. This can be valuable input to the management in the context of vulnerability of highland landscape to changing climatic condition affecting the ecosystem services and hence adaptive capacity of the natives.

We put forward that increase in vegetation cover at higher altitudes have changed surface temperature character resulting in warming. This can further threaten the melting of smaller glaciers at the higher altitude challenging the water supply system of a river basin putting the allied resource and services at risk.

STUDY AREA

The Satluj river is the longest tributary of the Indus River with the geographical extent of basin from 30°45' N to 33°00'N latitude to 76°15' E to 79°00' E longitude (Figure 1). It spreads within altitudinal range of 332m to 6558m. Covering an area of 18325 km^2 in Himachal Pradesh, it is geographically divided into Spiti valley, Tibet plateau, Khab to Nathpa, and Nathpa dam to Bhakhra Dam (R. Zhang et al., 2020) as upper, middle and lower Sutluj basin respectfully. It exhibits sub-humid tropical to arid temperate climate type and receives rainfall from western disturbances and heavy monsoon downpour as received in outer Himalayas. Heavy snowfall is also evident in Tibet plateau indicating most of the rainfall to be concentrated in the lower Satluj basin (Singh et al. 1997). The basin is known for variation in biodiversity due to variations in elevation. The Upper Satluj basin has less vegetation but a positive change is sort according to the India State of Forest Report 2021, where approximately 915 km^2 of the recorded forest area has shown an increase from 2019 data. The evidence for climate change is of 18.52% decline in snow cover during the year 2020 and 2021(Zhongming et al., 2021).

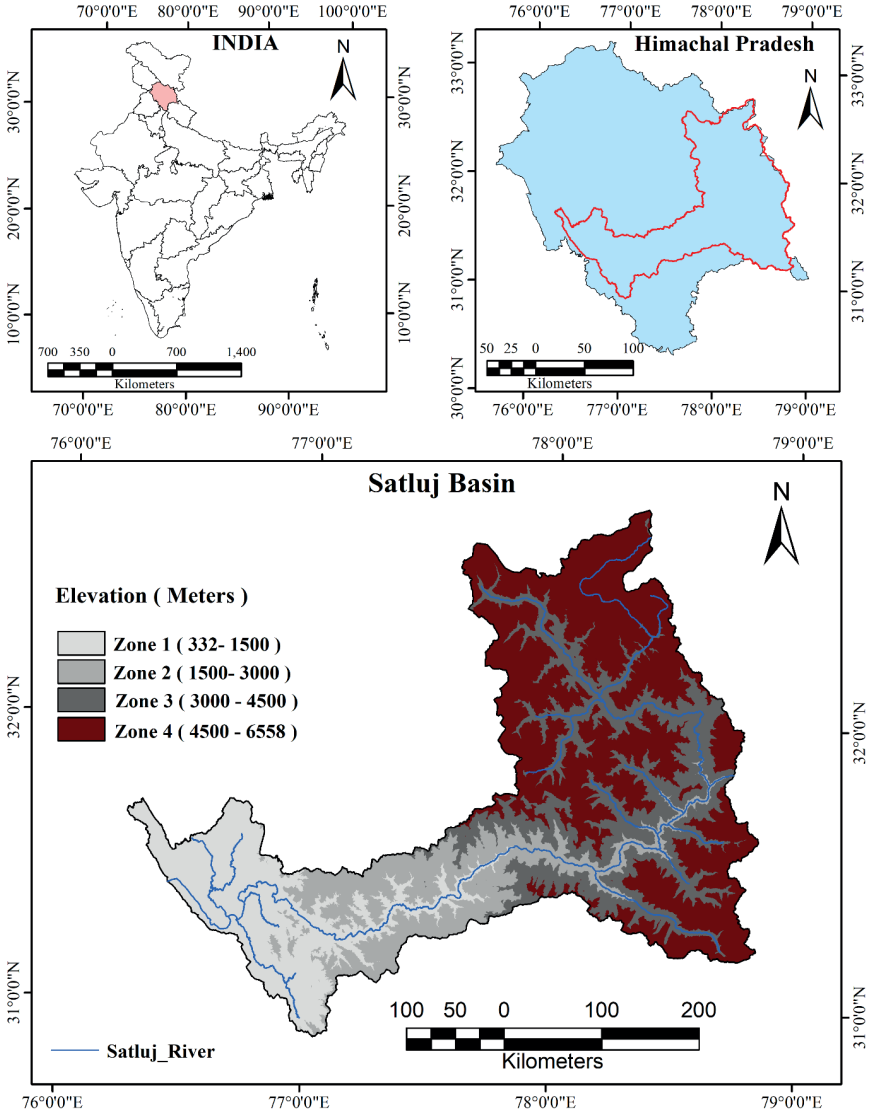

Fig. 1. Study area: Satluj Basin in Himachal Pradesh

METHODOLOGY

Datasets

To evaluate the land use change LANDSAT imageries were taken from the open-source data set available on the USGS website (https://earthexplorer.usgs.gov/) for 1980, 1996, 2011, and 2020 time periods (Table 1). The LST and NDVI were calculated for the years 1996, 2011, and 2020 due to weather appropriate availability of respected spectral bands in month of September and October. DEM (SRTM) 90M Resolution database (https://www.earthdata.nasa.gov/sensors/srtm)was utilized for analyzing the altitude wise change in land cover, LST, NDVI, and NDMI. ArcGIS environment was used for data retrieval, mapping, and analysis.

To ensure quality of data source an accuracy assessment of the 1980 LULC classification was done. The results of user and producer accuracy indicated that the highest classified LULC was recorded for snow cover for all the years. The Kappa coefficient evaluates the relative progress of the class over random assigning to classes (Pal et al. 2017), and the accuracy of the producer and user calculates the proportion of the map that is the correct pixel from the producer and user viewpoints. The average kappa coefficient was 0.79 and overall accuracy was 85.41% for 1996, 2011, and 2020 respectively. A kappa coefficient

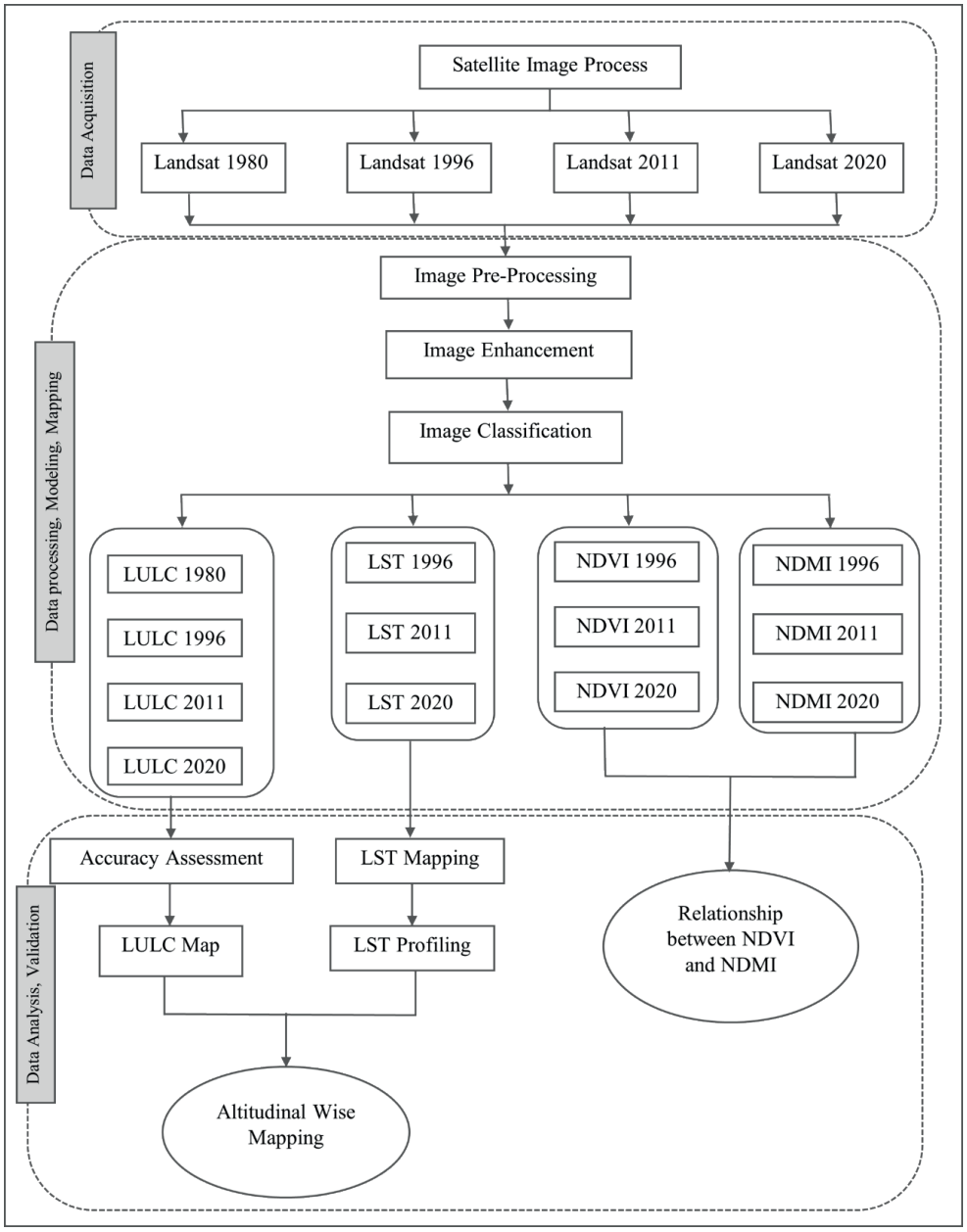

Fig. 2. Methodological framework for study

Table 1. Landsat datasets

Year	Satellite	Sensor	Acquisition Month	Path/Row	Spatial Resolution
1980	Landsat 3	1-5MSS	September-October	158/37,158/38,159/38, 157/38,158/39	80m
1996	Landsat 5	4-5TM	September-October	147/37,147/38,147/39,146/38	30m
2011	Landsat 5	4-5TM	September-October	147/37,147/38,147/39,146/38	30m
2020	Landsat 8	OLI	September-October	147/37,147/38, 146/38	30m

value greater than 0.7, indicates high conformity and is considered very good for research (Monserud et al. 1992). The confusion matrix was used for the accuracy of the LULC classification which is shown in Table 2.

LULC classifications

The LULC has been classified into 4 major classes namely, snow cover, vegetation, water body, and barren land. Supervised classification was done with the help of the Support Vector Machine (SVM) technique in ArcGIS 10.8. For testing and training of the SVMs model, detected that SVMs give reliable results with small training groups (Pal et al. 2006). In this study around 150 to 200 training samples for four classes were randomly taken from the LANDSAT imagery. The main benefits of SVM are that it creates less noise than other techniques and requires only a few training datasets for classification (Mountrakis et al. 2011).

Methods of LST computation from Landsat images

To calculate Land surface temperature from thermal image firstly the Digital Number (DN) is converted to Spectral Radiance (Lλ) utilizing equation 1 (Zhang et al. 2006).

$$L\lambda = \text{" } gain \text{ " } \times QCAL + \text{ " } offset \text{ "} \quad (1)$$

Where, *bias* = the intercept of the radiance/DN conversion function. *gain* =the slope of the radiance/DN conversion function *DN* =the digital number of a given pixel

The respective values are substituted in equation 1 as given in equation 2:

$$L\lambda = 0.037059 \times DN + 3.2 \quad (2)$$

The second step is regarding the conversion of spectral radiance to the brightness of satellite temperatures using equation 3 (Artis et al. 1982).

$$TB = \frac{K_2}{In\left(\frac{K_1}{L\lambda} + 1\right)} \quad (3)$$

Where K_1 and K_2 denote the correction constant in $Wm^{-2} sr^{-2} \mu m^{-2}$ (The value of K_2 is 1260.56 and K_1 is 607.76 for Landsat TM). TB is at-satellite brightness temperature (K), and L_λ is the Spectral radiance of the thermal band at radar aperture in $Wm^{-2} sr^{-2} \mu m^{-2}$.

The third step is At-satellite brightness temperature corrected by land surface emissivity (ε) therefore equation 4 was adopted (Snyder et al. 1998).

$$\varepsilon = 0.004 * Pv + 0.986 \quad (4)$$

Here, P_v denote as the Percentage of vegetation and it can be estimated using equation 5.

$$P_v = \left(\frac{NDVI_{jr} - NDVI_{MIN}}{NDVI_{MAX} + NDVI_{MIN}} \right) \quad (5)$$

The final step is a retrieval of Land Surface Temperature and it's computed following equation 6 (Artis et al. 1982).

$$LST = \frac{T_B}{\left[1 + \{ (\lambda \times TB/\rho) \times In\varepsilon \}\right]} \quad (6)$$

Where LST is the surface temperature (Kelvin), λ is the wavelength of produced radiance in meters (for which the highest reply and the regular of the preventive wavelengths (*λ=11.5μm* (Markham and Barker 1985) is utilized, $p=h*c/\sigma$ $(1.438*10^{-2} mK)$, σ is Boltzmann constant ($1.38*10^{-23} j/k$), h is indicated to Planck's constant ($6.626*10^{-34} J\ K^{-1}$) and ε= surface emissivity c is the velocity of light ($2.998*10^{8} m/s$). The conversion of surface temperature from Kelvin to degree Celsius (°C) 273 is done where 15 is subtracted from Eq.6 where 0 °C is equivalent to 273.15 K.

Calculation of NDVI and NDMI

The Normalized Difference Vegetation Index (NDVI) is estimated with help of Near and Visible Infrared Sensors (NIR & VIS) bands of satellite data (TOWNSHEND et al. 1986). NDVI is as follows:

NDVI = (NIR - VIS) / (NIR + VIS)

Normalized Difference Moisture Index (NDMI) is estimated with help of Near and Mid Infrared Bands (NIR & MIR) of satellite datasets(Jin et al. 2005). NDMI equation includes:

NDMI= (NIR-MIR) / (NIR+MIR)

RESULTS

Spatiotemporal Pattern of Land Use and Land Cover Changes

An evaluation of land use dynamics for a period of 40 years has been done. Figure 3 shows that barren land is the dominant land cover representation in the area which shows a decrease of 2.33 per cent since 1980 to 2020. Vegetation land cover represents the second largest leading class, ranging from 34.86 per cent (1980) to 42.49 per cent

Table 2. LULC Confusion Matrix

Year	1996		2011		2020	
LULC	U/A (%)	P/A (%)	U/A (%)	P/A (%)	U/A (%)	P/A (%)
Snow cover	96.42	100	95.45	95.45	88	100
Vegetation	91.89	70.83	96.42	79.41	100	75.51
Barren land	85.18	92	75	100	80	100
Water Body	65.78	83.33	77.14	79.41	76.31	87.87
Overall Accuracy	**83.84**		**85.74**		**86.66**	
Kappa Coefficient	**0.78**		**0.80**		**0.81**	

Where U/A and P/A indicate User accuracy and Producer accuracy respectively.

in 2020 (Table 3). It was continuously increasing over time, but was poorly represented in the initial observed years (1980-96 with meagre 3.47 per cent) but the second phase was high with 11 per cent positive change representing nearly 40 per cent of area covered under this category indicative of a 26-fold increase from 1980. The natural ecosystem dominant in higher latitudes by snow cover LULC class which decreased from 9.95 per cent of total area in 1980 to 4.35 per cent in 2020 whereas the water body has noted high perseverance from 131.26km^2 to 184.68km^2 over the period of analysis.

The dynamics of landscape across the study area showed heterogeneous patterns through time but still a geographic pattern can be sorted. The north and north eastern part of the region predominantly characterises decline in snow cover whereas the southern and south western part dominates with expansion of agricultural and vegetation area. The changed detection map has been produced from the post-classification of Land Sat imageries (1980–2020) for different LULC categories. After subtracting the total area of loss from the total gross gains, the net change of each landscape has been mapped (Figure 4). The conversion of barren land to vegetation cover (1642.92km^2) was more dominant in the area and was followed by snow cover to barren land (1084.83km^2) in the last 40 years.

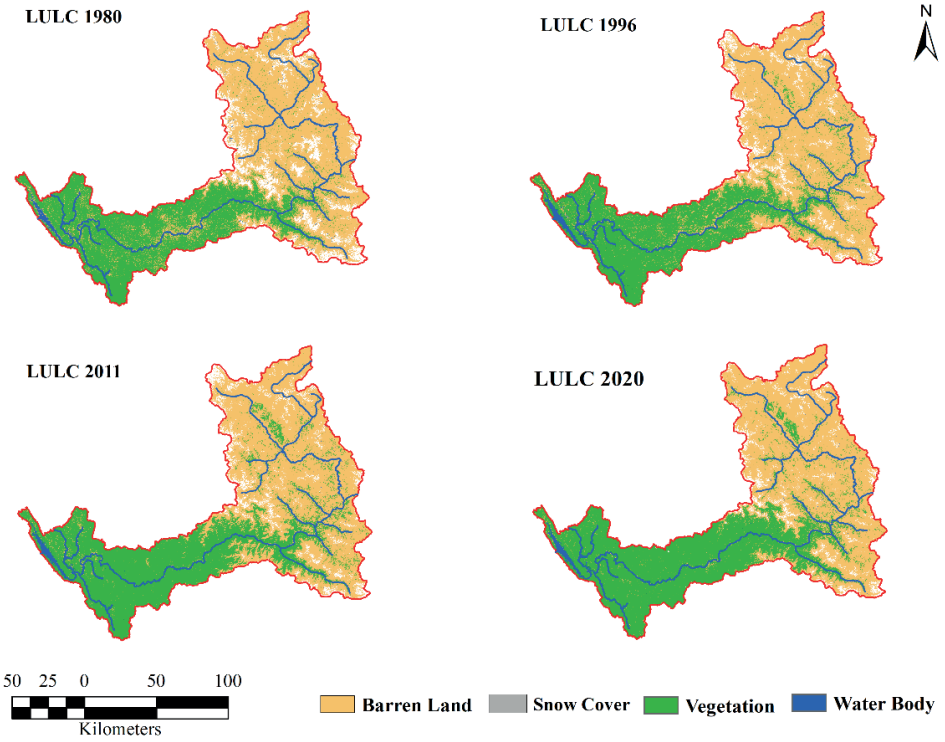

Fig. 3. Spatial pattern of LULC in the Satluj basin in 1980, 1996, 2011, and 2020

Table 3. Percentage of the LULC Area in different periods

LULC	1980 (Km^2)	Area in percentage	1996 (Km^2)	Area in percentage	2011 (Km^2)	Area in percentage	2020 (Km^2)	Area in percentage
Snow Cover	1823.22	9.95%	1042.42	5.69%	1017.06	5.54%	798.58	4.35%
Vegetation	6386.85	34.86%	6608.76	36.07%	7327.97	39.98%	7785.27	42.49%
Water Body	131.263	0.71%	211.09	1.15%	177.10	0.96%	184.68	1.00%
Barren Land	9977.73	54.46%	10456.64	57.08%	9805.86	53.50%	9550.39	52.13%

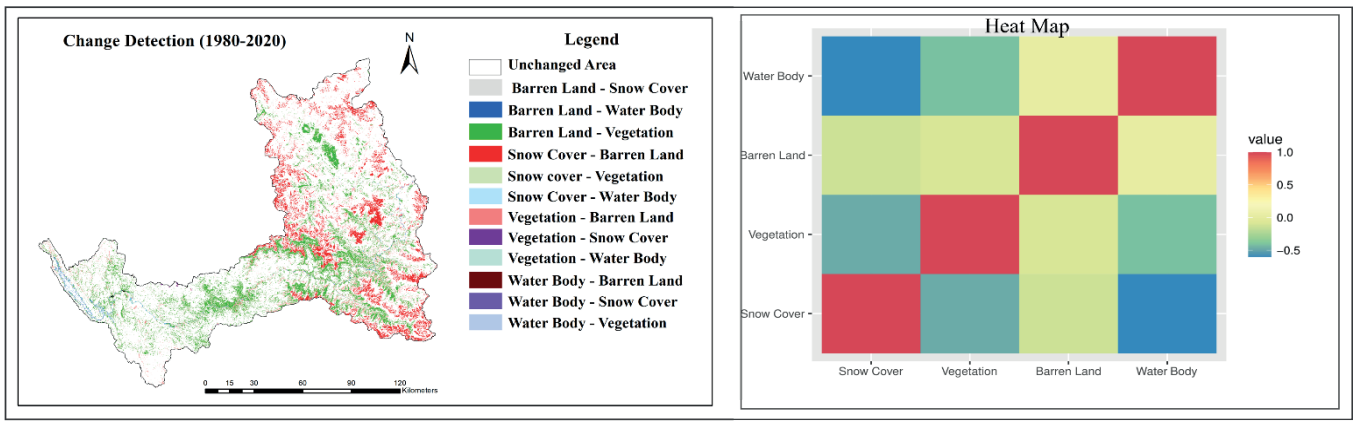

Fig. 4. Change detection map and Heat map of LULCC

LULC transitions along the altitude

The stability of respective classes of LULC is decreasing throughout the study period. The changes are more evident when studied along elevation bands. The study area is classified into four altitudinal zones based on SRTM DEM and delimited based on Natural Break in ArcGIS 10.8. Zone 1 is less than 1500 meters above sea level and is sub-tropical wet and consists of foothills and has more potential for the cultivation of cash crops such as paddy and off-season vegetables etc. Zone 2 is between 1500 and 3000 meters. Dense forest and high populated density are found in zone 1 and & 2. Zone 3 is between 3000 and 4500 meters, and zone 4 is higher than 4500 meters. Mostly Zone 3 & 4 are under high hilly and temperate dry region in Lahaul Spiti and Kinnaur district of state. Alphin vegetation, Glaciers, and low population density of state are found in these zones. Precipitation occurs from western disturbance and short warm summer in high altitude. Vegetation, water bodies, and barren land LULC classes are found in all four zones, and snow cover is found in only zones 3 and 4. Elevation plays an important role in the LULC changes because of rainfall and temperature variation. Temperature variations are influenced by many factors, including slope gradient and exposure.

Zone 1(Figure 5) is the area of lower basin of the Satluj river. Vegetation was dominated by LULC class at 2902.16km^2 (83.09%) but it increased over the area of 3205.82km^2 (91.73%) in 2020. Water bodies have increased by 3.05 per cent to 4.60 over the years from 1980 to 2020. The barren land area has drastically decreased from 483.54km^2 (13.84%) to 128km^2 (3.66%) in the last 40 years. It remained at only 3.66 per cent of the total area of zone 1in 2020.

Zone 2(Figure 5) is almost similar to Zone 1 where vegetation occupied 83.63 per cent of total area in 1980 and increased to 2749.83 sq. kms (93.67%) in 2020 whereas barren land decreased to almost 63.82 per cent of total area in the last four decades and the decreasing rate was high after 1996. This zone holds a smaller proportion of water bodies. Zone 3(Figure 5) is situated in the high-altitude and predominantly has snow cover showing a drastic decrease of 53.87km^2 in 1980 and to only 7.47km^2 in 2020 in absolute areal extend.

Zone 4 (Figure 5) is part of the upper Satluj basin. Snow cover and barren land were the most dominant LULC class in 1980, with 23.40 per cent and 75.20 per cent of total area respectively. Out of which the snow cover area decreased by 55.26 per cent, barren land slightly increased and occupied 15.51 per cent in last four decades. The vegetation area increased from 81.74km^2 to 198.43km^2 (142.75%) from 1980 to 2020. Vegetation is increasing in higher altitudes due to decreasing snow cover land is converting into barren land and rising surface temperature. It gives suitable conditions to grow shrubs in the higher altitude of the western Himalayas (Kumar et al., 2018).

Zones 3 and 4 were more vulnerable to change at higher altitudes (Figure 6). The conversion of barren land to vegetation cover is more dominant in Zone 3 from 1996–2011 and 2011–2020. In Zone 4, snow cover to barren land conversion is highest at 226.37km^2 (21.96%), and barren land to vegetation cover has converted to 174.35km^2 from 1996-2011. And the snow cover to barren land conversion rate was highest compared to the previous years, 2011–2020. It was 337.05km^2 (33.64%) in the last 10 years. The change in vegetation is prominent in all zones and notable for zone 3 and 4 in recent 15 years span. Within the reference period of 40 years long term positive change of more than 150 per cent in vegetation is evident in zone 4. The other landscape categories' conversion was lower with respect to their area. The rates of change of snow cover, vegetation, water body, and barren land in 4 different regions are shown in a table 4.

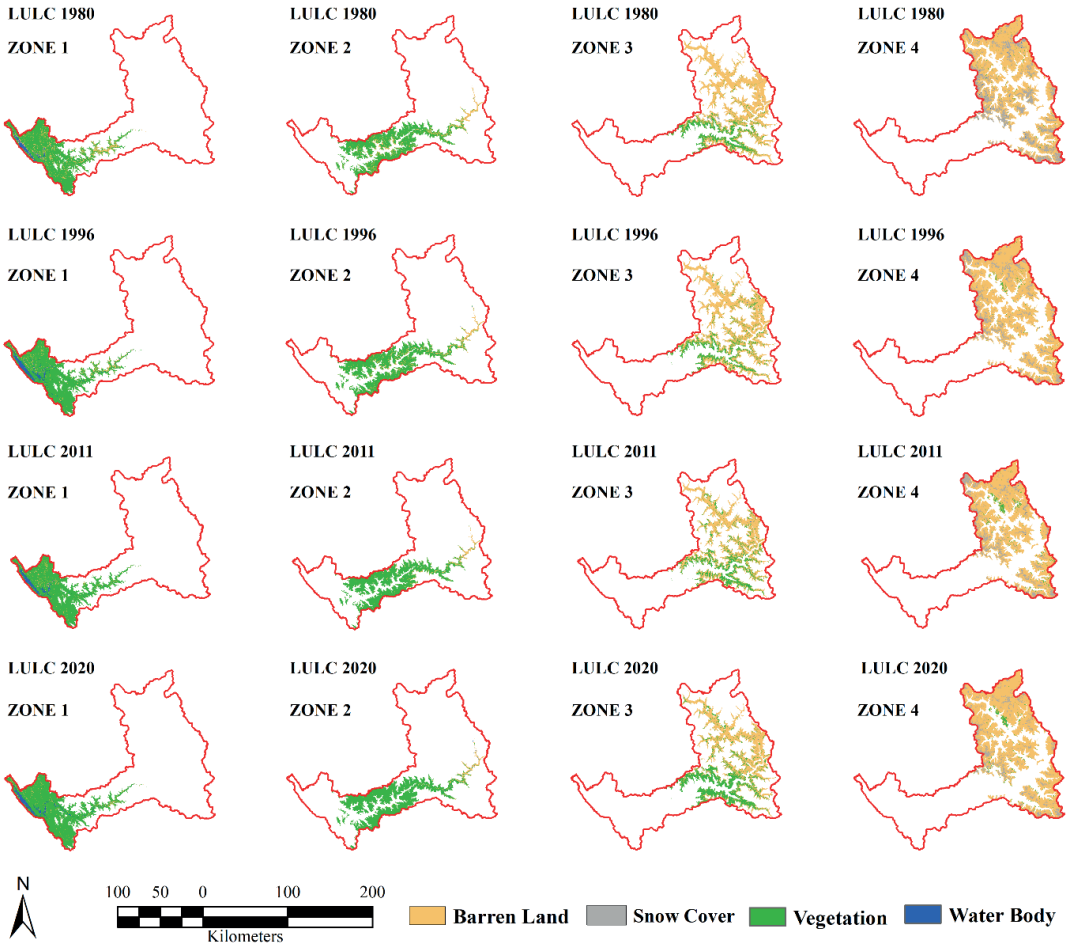

Fig. 5. Land cover change detection as per Elevation; Zone 1, Zone 2, Zone 3, Zone 4

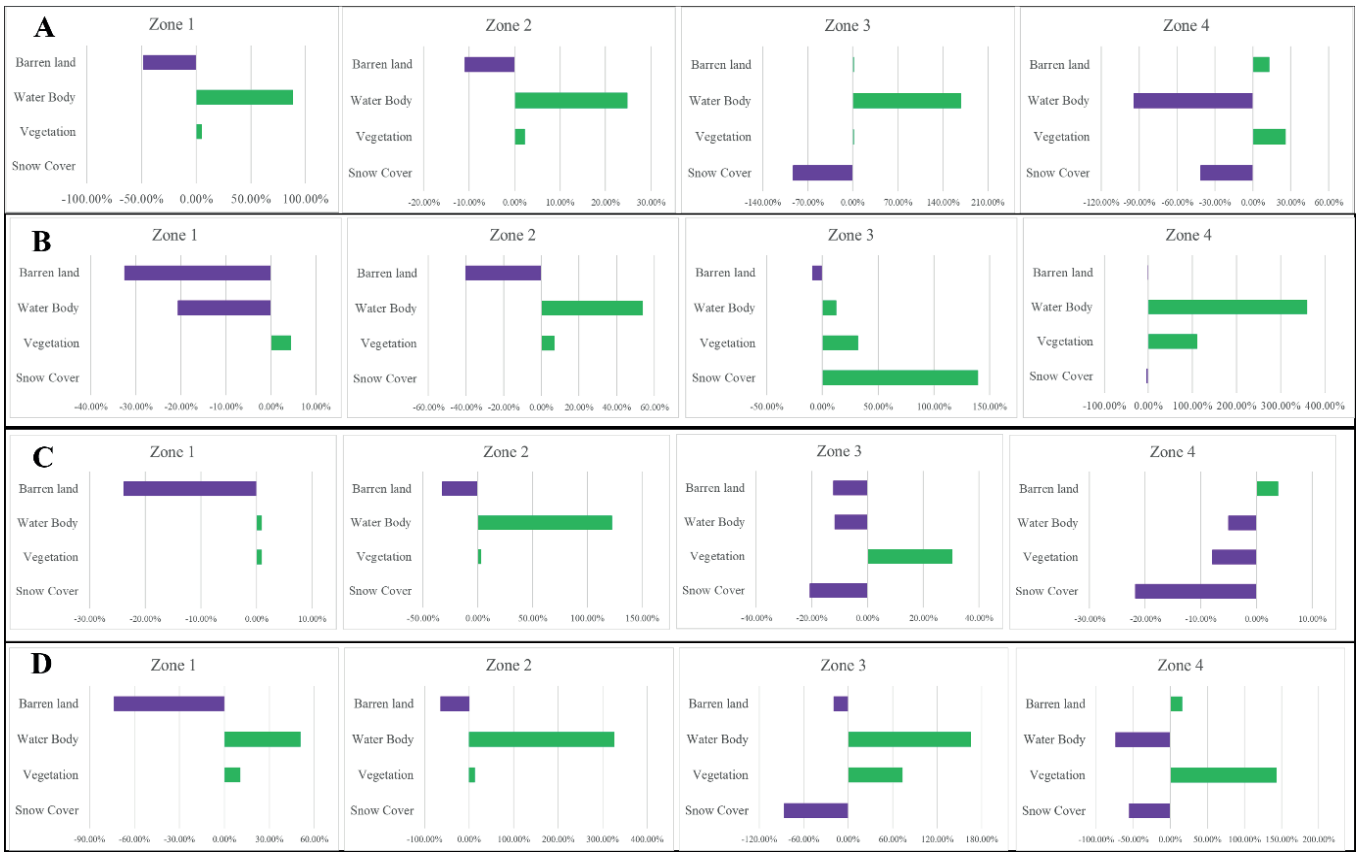

Fig. 6. Gain & Losses of LULC classes in percentage, A) 1980-1996, B) 1996-2011, C) 2011-2020, D) 1980-2020

Table 4. Rate of change (%) area under the different altitudinal-wise LULC

Zone	Class	1980-1996(%)	1996-2011(%)	2011-2020(%)	1980-2020(%)
Zone 1	Snow cover	0	0	0	0
	Vegetation	4.94	4.33	0.88	10.46
	Water Body	88.16	-20.63	0.87	50.64
	Barren Land	-48.53	-32.49	-23.8	-73.52
Zone 2	Snow cover	0	0	0	0
	Vegetation	2.19	6.84	2.68	12.12
	Water Body	24.91	53.8	121.84	326.22
	Barren Land	-10.87	-40.05	-32.3	-63.82
Zone 3	Snow cover	-92.7	139.44	-20.61	-86.13
	Vegetation	0.95	31.4	30.29	72.84
	Water Body	168.1	12.09	-11.69	165.4
		1.12	-9.08	-12.15	-19.23
Zone 4	Snow cover	-41.13	-2.89	-21.73	-55.26
	Vegetation	25.71	109.712	-7.92	142.75
	Water Body	-94.03	361.94	-5	-73.8
	Barren Land	12.88	-1.43	3.82	15.51

Transitions of native vegetation ecosystem

In general, the stability of vegetation is increasing over the study period across the river basin (Figure 7), with increasing traces of open forest above 4500 m, primarily in the Spiti valley and Kinnaur district. The sparse vegetation which was 26.74% in 1996 and increased to 41.55% of the total forest area as estimated from values of NDVI which is approx. 0.39 (1996) to 0.31(2020) in higher altitude. This is an indicator of decrease in reflectance from the available green cover hence decrease of its spatial extent. Native forest density is also decreasing in the entire river basin.

The total dense forest area has reduced from 119.72km^2 to almost null value (table 5). As evident from table the scale of representation of NDVI highest value has reduced from 0.75 (1996) to 0.61 (2020). The spatial extent of decrease in the range is much evident in lower altitude of the basin in less than 4500m. Figure 7 shows the decrease in south western part in district of Bilaspur, Mandi. The possible explanation would be change to open forest type (Table 5). The barren land of LULC class has been changed to vegetation area (approximately 1642.92km^2) and snow cover class has also changed to vegetation covering around 13.65km^2 in the study period. The early trace of open vegetation types is found in upper river basin (Figure7).

Spatiotemporal pattern of LST

The spatiotemporal pattern of LST was vital for considering to evaluate the influence of changes in mountain land use. LST deducts the radiative skin temperature produced from the earth's surface, including bare earth, paved surfaces, building roofs, vegetation, and water (Voogt et al. 2003). The thermal map was produced by using Landsat imagery of 1996, 2011, and 2020 (Figure 8). The mean LST of the Satluj basin was noted as 10.3°C in 1996, but it increased by more than 2°C and reached 13.64°C in 2011. In the latter half of the study LST rapidly increased to reach 16.55°C in 2020.

When evaluated based on elevation zones we found that zone 1 existed above the 10°C temperature range (Figure 10). The result shows that the 10°C to 20°C LST belt area is moving towards the 20°C to 30°C LST belt as evaluated during 1996 to 2020 (Figure 10). The area representing more than 30°C in zone 1 was 2.17 km^2 in 1996, but it increased about forty-fold in 25 years (Figure 10). In zone 2, meagre area is recorded under the 0°C LST whereas the 0°C to 10°C temperature belt almost disappeared from 1996 to 2020 (Figure 9, Figure 10). The mean LST of zone 2 was 15.85°C, 17.10°C, and 20.06°C in 1996, 2011, and 2020 respectively.

Zones 3 and 4 are situated in the high altitudinal zone. The results show that zone 3 is more sensitive to changes in LST. The area under less than -10 °C temperature was 49.97 km2 in 1996 reduced to 2.5 km2 in 2011 and none of it extend were traceable in 2020 (Figure 9, Figure 10). From 1996 to 2020, zone 4 mean LST increased more than zone 3.

Transition pattern of NDMI

The NDMI indicates the characteristic of earth vegetation dynamics and is closer to tracking changes in plant biomass (Delgado et al. 2022; Jin et al. 2005) The results of the NDMI calculation ranged from 0.96 to -0.95 in 1996 and 0.95 to -0.81 in 2011, but it rapidly changed after 2011, from 0.73 to -0.43 in 2020 (Figure 11). It can be understood from the map that a snow-covered area is present at a high altitude. NDMI values are low, the same as NDVI values in the lower river basin of 2020. The variation in NDMI values can see in (figure 11).

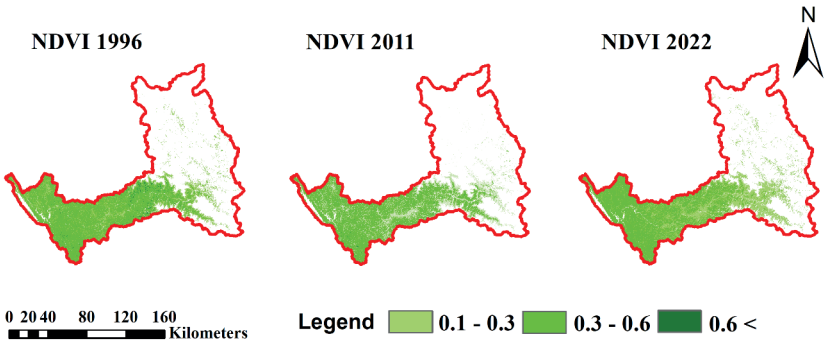

Fig. 7. Spatial pattern of NDVI in 1996, 2011, and 2020

Table 5. Matrix of type of Vegetation

Vegetation/Year	1996 (km^2)	2011 (km^2)	2022 (km^2)
Open Vegetation (0.1-0.3)	2014.47	2307.75	**3213.67**
Moderate Vegetation (0.3-0.6)	5398.99	5096.28	4519.58
Dense Vegetation (More than 0.6)	119.72	27.31	0.0018

*Bold value denotes positive change

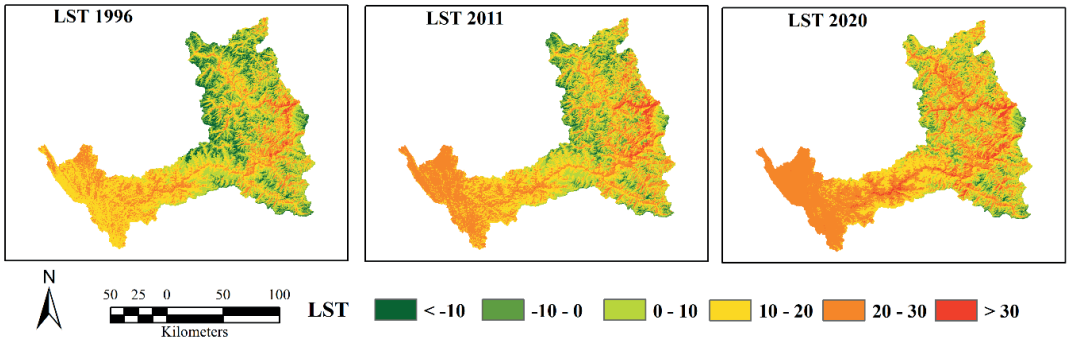

Fig. 8. Spatio-temporal pattern of LST in 1996, 2011, and 2020

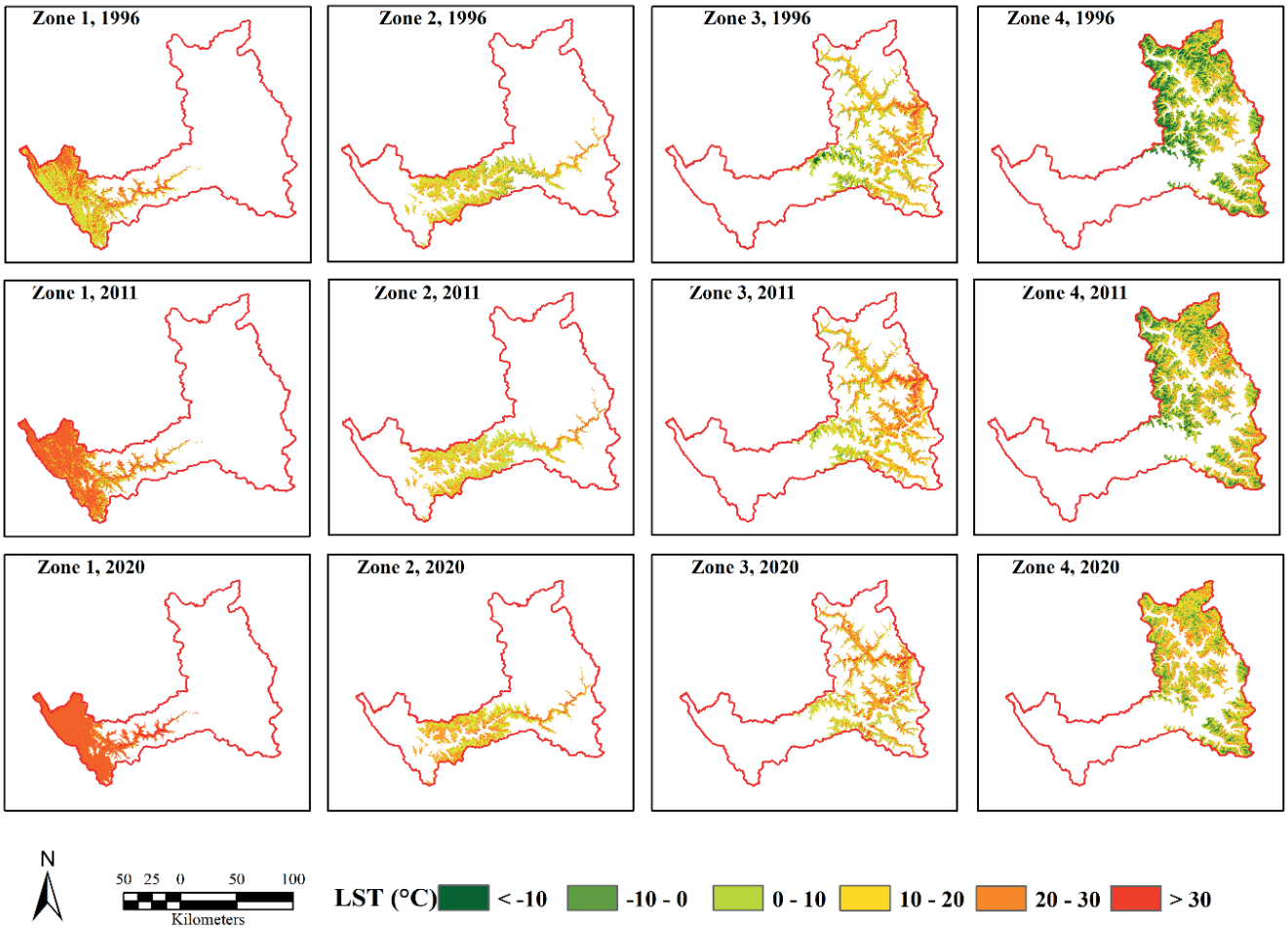

Fig. 9. Map of LST detection along altitudinal zones

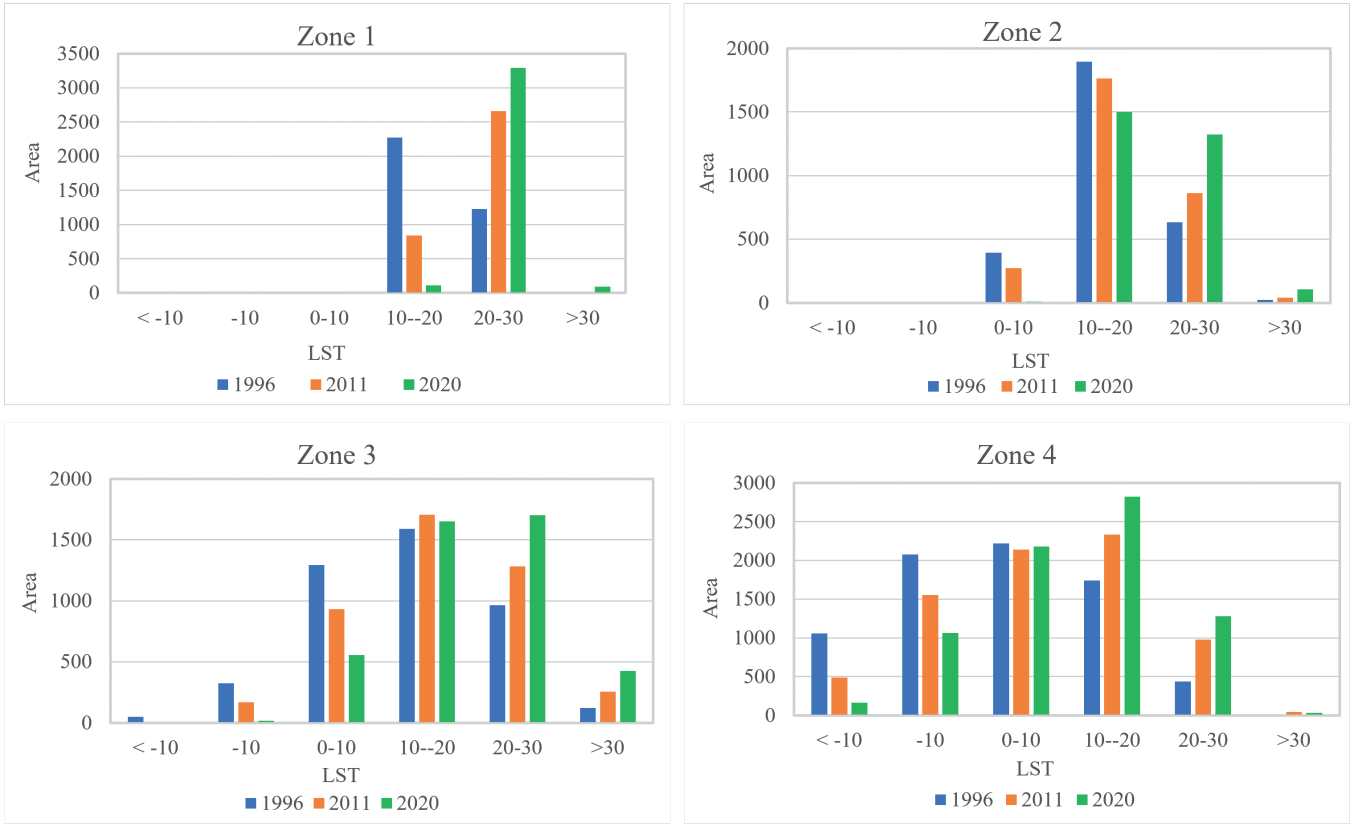

Fig. 10. Bar plot of LST area change along with elevation

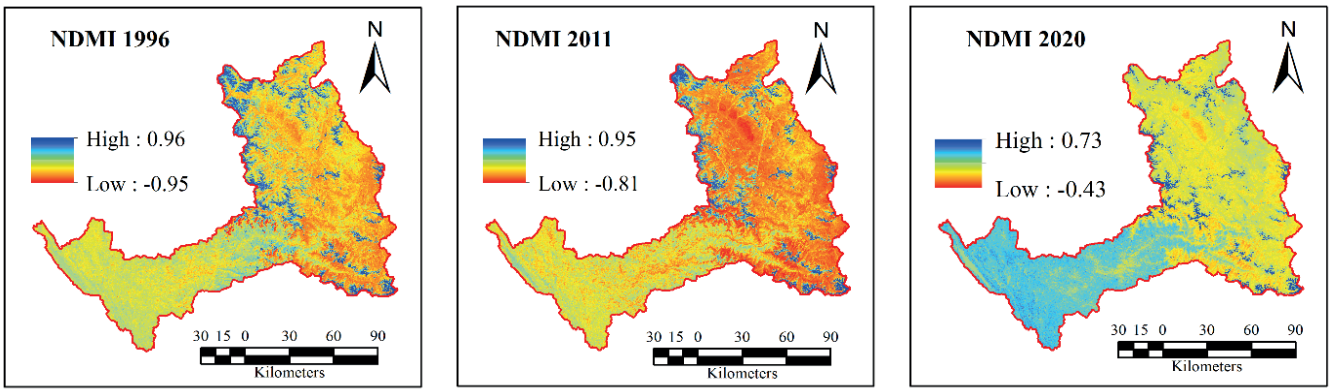

Fig. 11. Spatial pattern of NDMI in 1996, 2011, and 2020 in the study area

DISCUSSION

Temperature variation for different elevation-based zones

Our research finding indicate significantly steady growth in land use change and surface temperature in over the year but this trends more prominent in recent decades. This similar trend also finds in pervious study in Himalayan regions (Khan et al., 2023; Satti et al., 2023). The relationship between LULC and LST along elevation was investigated using a graphical LST profile, which provides a better comprehensive understanding of the dynamics change of LST. Two cross-section lines have been made to obtain each pixel value of LST where zone wise LST was shown, A-B represents all four zones, and C-D represents only zones 3 and 4 (Figure 12). When we see surface temperatures between all LULC types, the LST has profoundly increased across elevation zones. It is found from the cross profile that barren land recorded high LST in all zones (25-27°C in 1996, 29-32°C in 2011, and 33-36°C in 2020), and water bodies recorded the lowest LST in lower attitude (17-19°C in 1996, 21-22°C, 24-25°C in 2020).

The observed trend from the result of LULC reveals that the mean temperature of all zones increased. The probable explanation would be the decrease in forest density and the snow cover at higher altitudes. As per the LST profile map A-B (Figure 12), zone 1 mean temperature was recorded at 19.32°C in 1996 and it increased by 4.4°C (23.72°C) in the last 24 years. The same is evident in zone 2 where the mean surface temperature that was 15.85°C recorded in 1996 increased nearly 4.21°C (17.10°C in 2011 and 20.06°C in 2020) from 1996 to 2020. The spectrally quantified index value demonstrates decreasing density of vegetation with increase in LST (Shahfahad et al., 2020). Several similar studies indicate that snow, vegetation, and water bodies have relatively lower temperatures, whereas sparse vegetation and bare earth have higher temperatures (Das et al. 2020; Kumar et al. 2018; Njoku et al. 2022; Worku et al. 2021).

The snow cover area has decreased but its annual fluctuation is also evident in various studies in the Himalayan region (Haq et al. 2020; Maurya et al. 2021). In our study the LST profile shows that zones 3 and 4 are more vulnerable to changes in LULC and LST. The mean surface temperature for zone 3 & 4 was the had the highest positive increase of 6.46°C during the study period (12.91°C in 1996, 16.10°C in 2011, and 19.37°C in 2020) and 7.59°C (2.73°C in 1996, 7.38°C in 2011, and 19.37°C in 2020) in last 24 years respectively. It has been observed that the highest LST change (Figure 12, C-D) is complementing the decreasing snow cover area and increasing barren land. The changes in the sample LST value for the same vegetation cover pixel was calculated and a progressive increase was evident (18-19°C in 1996, 22-23°C in 2011, and 26-27°C in 2020) in the higher altitude. The ongoing degradation of mountain ecosystem due to anthropogenic pressure and global climate change in the Himalaya region and similar trend also found in the Alpe, Rocky and other global Mountains in several research studies (F. Zhang et al., 2022; H. Zhang et al., 2022). Further the same sample was correlated with NDMI value. A significant correlation was found between NDVI and NDMI (Figure 13).

The Linear Regression between NDVI and NDMI denotes a positive correlation with the correlation coefficient of R^2 = 0.4077, R^2 = 0.5523, and R^2 = 0.6995 in 1996, 2011, and 2020, respectively, indicating that vegetation content has increased along with moisture content over the study period (Figure 13).

The further scenario is not estimating the beyond the scope of the study but that would be taken further with help of modelling tool such as the InVEST model for examine the habitat quality, water balance for river ecosystem. The recognized changed in vegetation are positive way for local communities' livelihood. Agriculture pattern is changed in higher altitude such as apples, potato and etc. farming are altitudinal shifting in this region because global climate change gives suitable condition for this practice and plantation program results are shown in the Spiti region.

CONCLUSION

This study assessed the spatial pattern of LULC change and LST in the Satluj basin, Himachal Pradesh from 1980-2020. It analyzed the dynamics of LULC and LST with changing elevation based on altitudinal zonation of the landscape. The LULC was divided into different classes like vegetation, snow cover, barren land, and water bodies and was evaluated with help of the Support Vector Machine. The results of LULC denote that the Satluj basin has undergone change since 1980. Snow cover has decreased by 56.19% and vegetation cover has increased by 21.89% within the same study period. The spatial and temporal pattern of LST also evidently mark its dynamics in the river basin. The analyses demonstrates that the mean surface temperature of the Satluj basin has amplified by about 0.25°C per year since 1996 and has increased 60.67 per cent (10.3°C to 16.55°C) in the last 24 years. Altitude wise zonation of LST exhibits an increase of 0.18°C/year in zone 1, 0.17°C /year in zone 2, 0.26°C/year in zone 3, and 0.31°C/year in zone 4 respectively. The analyses of this study recommend that LST can be the key factor to LULC character of the landscape. The decrease in NDVI values show the transition in native vegetation. The characteristic expansion in sparse vegetation area and decrease in terms of vegetation density is well evident from the study. Due to the increase in LST and melting of snow cover,

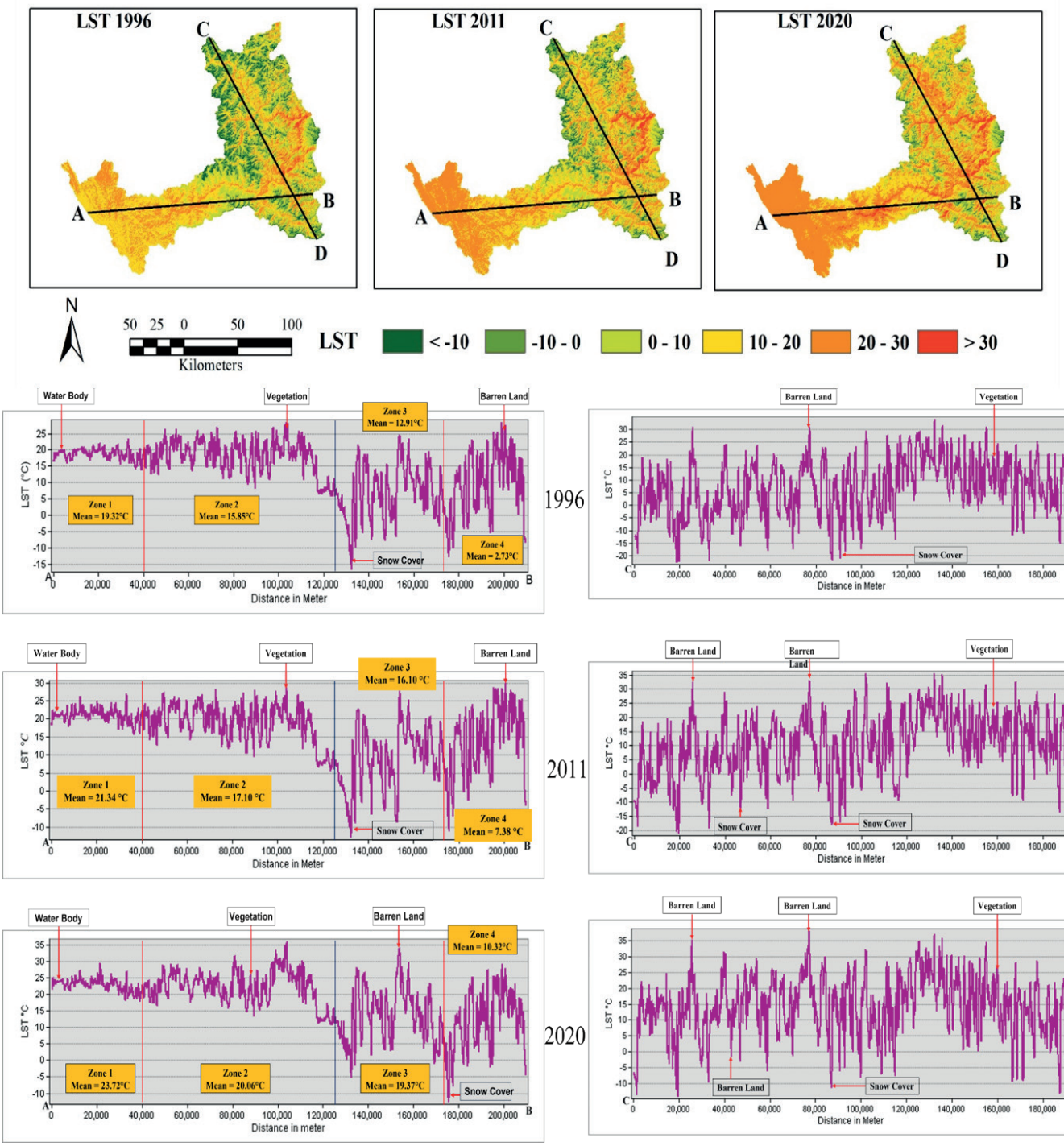

Fig. 12. LST profile (A-B; C-D) over the LST of 1996, 2011, and 2020

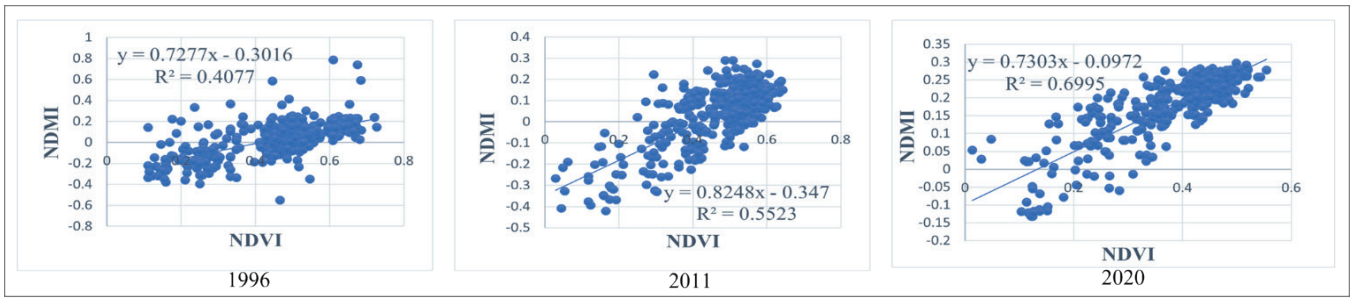

Fig. 13. Correlation between NDVI and NDMI

conditions in the high altitudinal zone are favourable for growth of sparse vegetation. Changing global climate and land transformation have a both positive and negative consequences for the local community. Melting snow would be create water scarcity problem in next coming decades but increasing vegetation land are enhancing local community economy through develop market for the farmers crops. Tourism activity also increase in this region that help in positive way to local community livelihood. Decreasing vegetation density status have strong impact on forest function, biodiversity and sustainability of local people in lower river basin.

Land transformation and LST can change the mountain climate and ecological balance. Society is totally defending on the ecosystem services in the Himalayan Mountain. Change in global climate and anthropogenic pressure have impact on ecosystem services such as water balance, soil quality, food production, habitat quality and carbon storage etc. Many natural disasters can occur such as floods, Glacial Lake Outburst flood, landslides due to environmental change. These changes make difficult to sustain livelihood of community. All these circumstances can lead to migration from mountain region to other place and can be create environmental refuge and disturbance in demographic dividend.

Our study revealed that the potential impact of land transformation and climate change on river basin is becoming a significant issue for all stockholders such as policymakers, local community, river basin engineers, etc. The deterioration of natural resource has increasing vulnerability of local community to absorb shock of frequent natural events due climate change. These results help the identification of potential priority region for more vulnerable exposure level to multiple pressure for the future monitoring activities and decision makers to mitigate possible impact from anthropogenic intervention. Local government authorities can propose better climate risk adaptation plan at attitudinal zone level for the farmers and local community to prevent the global climate change on basis of study findings.

REFERENCES

Ali, S. A., Khatun, R., Ahmad, A., & Ahmad, S. N. (2019). Application of GIS-based analytic hierarchy process and frequency ratio model to flood vulnerable mapping and risk area estimation at Sundarban region, India. Modeling Earth Systems and Environment, 5(3), 1083–1102. https://doi.org/10.1007/s40808-019-00593-z

Artis, D. A., & Carnahan, W. H. (1982). Survey of Emissivity Variability in Thennography of Urban Areas. 329, 313–329. https://doi.org/10.1016/0034-4257(82)90043-8.

Bandyopadhyay, D., Mukherjee, S., Singh, G., & Coomes, D. (2023). The rapid vegetation line shift in response to glacial dynamics and climate variability in Himalaya between 2000 and 2014. Environmental Monitoring and Assessment, 195(1). https://doi.org/10.1007/s10661-022-10577-9

Bindajam, A. A., Mallick, J., Alqadhi, S., & Singh, C. K. (n.d.). Impacts of Vegetation and Topography on Land Surface Temperature Variability over the Semi-Arid Mountain Cities of Saudi Arabia. 1–28. Atmosphere, 11(7), 762. https://doi.org/10.3390/ATMOS11070762.

Chauhan, N., Upadhyay, S. K., & Singh, R. (2021). The Himalayan natural resources: Challenges and conservation for sustainable development. Article in Journal of Pharmacognosy and Phytochemistry, 10(1), 1643–1648. www.phytojournal.com

Chhogyel, N., Kumar, L., Bajgai, Y., & Hasan, M. K. (2020). Perception of farmers on climate change and its impacts on agriculture across various altitudinal zones of Bhutan Himalayas. International Journal of Environmental Science and Technology, 17(8), 3607–3620. https://doi.org/10.1007/s13762-020-02662-8

Das, S., & Angadi, D. P. (2020). Land use-land cover (LULC) transformation and its relation with land surface temperature changes: A case study of Barrackpore Subdivision, West Bengal, India. Remote Sensing Applications: Society and Environment, 19(July 2019), 100322. https://doi.org/10.1016/j.rsase.2020.100322

Delgado-Moreno, D., & Gao, Y. (2022). Forest Degradation Estimation Through Trend Analysis of Annual Time Series NDVI, NDMI and NDFI (2010–2020) Using Landsat Images BT - Advances in Geospatial Data Science (R. Tapia-McClung, O. Sánchez-Siordia, K. González-Zuccolotto, & H. Carlos-Martínez (eds.); pp. 149–159). Springer International Publishing.

Grêt-Regamey, A., Weibel, B., Bagstad, K. J., Ferrari, M., Geneletti, D., Klug, H., Schirpke, U., & Tappeiner, U. (2014). On the effects of scale for ecosystem services mapping. PLoS ONE, 9(12), 1–26. https://doi.org/10.1371/journal.pone.0112601

Haq, M. A., Baral, P., Yaragal, S., & Rahaman, G. (2020). Assessment of trends of land surface vegetation distribution, snow cover and temperature over entire Himachal Pradesh using MODIS datasets. Natural Resource Modeling, 33(2). https://doi.org/10.1111/nrm.12262

Holzman, M. E., Rivas, R., & Piccolo, M. C. (2014). Estimating soil moisture and the relationship with crop yield using surface temperature and vegetation index. International Journal of Applied Earth Observation and Geoinformation, 28(1), 181–192. https://doi.org/10.1016/j.jag.2013.12.006

Husain, M. A., Kumar, P., Singh, A., Raman, V. A. V, Dua, R., & Thakur, S. (2023). Snow Cover and Snowline Variation in Relation to Land Surface Temperature in Spiti Valley, Himachal Pradesh, India. International Journal of Ecology and Environmental Sciences, 49, 187–199.

Jin, S., & Sader, S. A. (2005). Comparison of time series tasseled cap wetness and the normalized difference moisture index in detecting forest disturbances. Remote Sensing of Environment, 94(3), 364–372. https://doi.org/10.1016/j.rse.2004.10.012

John, A., Cannistra, A. F., Yang, K., Tan, A., Shean, D., Hille Ris Lambers, J., & Cristea, N. (2022). High-Resolution Snow-Covered Area Mapping in Forested Mountain Ecosystems Using PlanetScope Imagery. Remote Sensing, 14(14), 1–24. https://doi.org/10.3390/rs14143409

Khan, A., Haque, S. M., & Biswas, B. (2023). Altitudinal Shifting of Apple Orchards with Adaption of Changing Climate in the Alpine Himalaya. Journal of the Indian Society of Remote Sensing, 51(5), 1135–1155. https://doi.org/10.1007/s12524-023-01678-0

Kumar, P., Husain, A., Singh, R. B., & Kumar, M. (2018). Impact of land cover change on land surface temperature: A case study of Spiti Valley. Journal of Mountain Science, 15(8), 1658–1670. https://doi.org/10.1007/s11629-018-4902-9

Li, Z., Jia, L., & Lu, J. (2015). On uncertainties of the Priestley-Taylor/LST-Fc feature space method to estimate evapotranspiration: Case study in an arid/semiarid region in northwest China. Remote Sensing, 7(1), 447–466. https://doi.org/10.3390/rs70100447

Lutz, A. F., Immerzeel, W. W., Gobiet, A., Pellicciotti, F., & Bierkens, M. F. P. (2013). Comparison of climate change signals in CMIP3 and CMIP5 multi-model ensembles and implications for Central Asian glaciers. Hydrol. Earth Syst. Sci., 17(9), 3661–3677. https://doi.org/10.5194/hess-17-3661-2013

MARKHAM, B. L., & BARKER, J. L. (1985). Spectral characterization of the LANDSAT Thematic Mapper sensors. International Journal of Remote Sensing, 6(5), 697–716. https://doi.org/10.1080/01431168508948492

Maurya, R., Negi, V. S., & Pandey, B. W. (2021). Spatio-temporal analysis of land use/land cover change through overlay technique in Kinnaur district of Himachal pradesh, Western Himalaya. Sustainability, Agri, Food and Environmental Research, 9(1). https://doi.org/10.7770/safer-v0n0-art2161

Monserud, R. A., & Leemans, R. (1992). Comparing global vegetation maps with the Kappa statistic. Ecological Modelling, 62(4), 275–293. https://doi.org/10.1016/0304-3800(92)90003-W

Mountrakis, G., Im, J., & Ogole, C. (2011). Support vector machines in remote sensing: A review. ISPRS Journal of Photogrammetry and Remote Sensing, 66(3), 247–259. https://doi.org/10.1016/j.isprsjprs.2010.11.001

Njoku, E. A., & Tenenbaum, D. E. (2022). Remote Sensing Applications : Society and Environment Quantitative assessment of the relationship between land use / land cover (LULC), topographic elevation and land surface temperature (LST) in Ilorin , Nigeria. Remote Sensing Applications: Society and Environment, 27, 100780. https://doi.org/10.1016/j.rsase.2022.100780

Pal, M., & Mather, P. M. (2006). Some issues in the classification of DAIS hyperspectral data. International Journal of Remote Sensing, 27(14), 2895–2916. https://doi.org/10.1080/01431160500185227

Pal, S., & Ziaul, S. (2017). Detection of land use and land cover change and land surface temperature in English Bazar urban centre. Egyptian Journal of Remote Sensing and Space Science, 20(1), 125–145. https://doi.org/10.1016/j.ejrs.2016.11.003

Pang, G., Chen, D., Wang, X., & Lai, H. W. (2022). Spatiotemporal variations of land surface albedo and associated influencing factors on the Tibetan Plateau. Science of the Total Environment, 804, 150100. https://doi.org/10.1016/j.scitotenv.2021.150100

Rani, S., & Mal, S. (2022). Trends in land surface temperature and its drivers over the High Mountain Asia. Egyptian Journal of Remote Sensing and Space Science, 25(3), 717–729. https://doi.org/10.1016/j.ejrs.2022.04.005

Roy, P. S., Ramachandran, R. M., Paul, O., Thakur, P. K., Ravan, S., Behera, M. D., Sarangi, C., & Kanawade, V. P. (2022). Anthropogenic Land Use and Land Cover Changes—A Review on Its Environmental Consequences and Climate Change. Journal of the Indian Society of Remote Sensing, 50(8), 1615–1640. https://doi.org/10.1007/s12524-022-01569-w

Satti, Z., Naveed, M., Shafeeque, M., Ali, S., Abdullaev, F., Ashraf, T. M., Irshad, M., & Li, L. (2023). Effects of climate change on vegetation and snow cover area in Gilgit Baltistan using MODIS data. Environmental Science and Pollution Research, 30(7), 19149–19166. https://doi.org/10.1007/s11356-022-23445-3

Shahfahad, Kumari, B., Tayyab, M., Ahmed, I. A., Baig, M. R. I., Khan, M. F., & Rahman, A. (2020). Longitudinal study of land surface temperature (LST) using mono- and split-window algorithms and its relationship with NDVI and NDBI over selected metro cities of India. Arabian Journal of Geosciences, 13(19). https://doi.org/10.1007/s12517-020-06068-1

Singh, P., & Kumar, N. (1997). Impact assessment of climate change on the hydrological response of a snow and glacier melt runoff dominated Himalayan river. Journal of Hydrology, 193(1–4), 316–350. https://doi.org/10.1016/S0022-1694(96)03142-3

Snyder, W. C., & Wan, Z. (1998). BRDF models to predict spectral reflectance and emissivity in the thermal infrared. IEEE Transactions on Geoscience and Remote Sensing, 36(1), 214–225. https://doi.org/10.1109/36.655331

Swain, S., Mishra, S. K., Pandey, A., & Kalura, P. (2022). Inclusion of groundwater and socio-economic factors for assessing comprehensive drought vulnerability over Narmada River Basin, India: A geospatial approach. Applied Water Science, 12(2), 1–16. https://doi.org/10.1007/s13201-021-01529-8

Taripanah, F., & Ranjbar, A. (2021). Quantitative analysis of spatial distribution of land surface temperature (LST) in relation Ecohydrological, terrain and socio- economic factors based on Landsat data in mountainous area. Advances in Space Research, 68(9), 3622–3640. https://doi.org/10.1016/j.asr.2021.07.008

TOWNSHEND, J. R. G., & JUSTICE, C. O. (1986). Analysis of the dynamics of African vegetation using the normalized difference vegetation index. International Journal of Remote Sensing, 7(11), 1435–1445. https://doi.org/10.1080/01431168608948946

Upadhayaya, P. K. (2015). Sustainability Threats to Mountain Tourism with Tourist Mechanized Mobility Induced Global Warming: A Case Study of Nepal. Journal of Tourism & Hospitality, 04(02). https://doi.org/10.4172/2167-0269.1000148

Vannier, C., Lasseur, R., Crouzat, E., Byczek, C., Lafond, V., Cordonnier, T., Longaretti, P. Y., & Lavorel, S. (2019). Mapping ecosystem services bundles in a heterogeneous mountain region. Ecosystems and People, 15(1), 74–88. https://doi.org/10.1080/26395916.2019.1570971

Voogt, J. A., & Oke, T. R. (2003). Thermal remote sensing of urban climates. Remote Sensing of Environment, 86(3), 370–384. https://doi.org/10.1016/S0034-4257(03)00079-8

Wen, X. (2020). Temporal and spatial relationships between soil erosion and ecological restoration in semi-arid regions: a case study in northern Shaanxi, China. GIScience and Remote Sensing, 57(4), 572–590. https://doi.org/10.1080/15481603.2020.1751406

Worku, G., Teferi, E., & Bantider, A. (2021). Assessing the effects of vegetation change on urban land surface temperature using remote sensing data: The case of Addis Ababa city, Ethiopia. Remote Sensing Applications: Society and Environment, 22(April), 100520. https://doi.org/10.1016/j.rsase.2021.100520

Xystrakis, F., Psarras, T., & Koutsias, N. (2017). A process-based land use/land cover change assessment on a mountainous area of Greece during 1945–2009: Signs of socio-economic drivers. Science of the Total Environment, 587–588, 360–370. https://doi.org/10.1016/j.scitotenv.2017.02.161

Young, K. R. (2014). Ecology of land cover change in glaciated tropical mountains. Revista Peruana de Biología, 21(3), 259–270.

Zhang, F., Zeng, B., Yang, T., Zheng, Y., & Cao, Y. (2022). A Multi-Perspective Assessment Method with a Dynamic Benchmark for Human Activity Impacts on Alpine Ecosystem under Climate Change. Remote Sensing, 14(1). https://doi.org/10.3390/rs14010208

Zhang, H., Zhan, C., Xia, J., & Yeh, P. J. F. (2022). Responses of vegetation to changes in terrestrial water storage and temperature in global mountainous regions. Science of the Total Environment, 851(July), 158416. https://doi.org/10.1016/j.scitotenv.2022.158416

Zhang, J., Wang, Y., & Li, Y. (2006). A C++ program for retrieving land surface temperature from the data of Landsat TM/ETM+ band6. Computers and Geosciences, 32(10), 1796–1805. https://doi.org/10.1016/j.cageo.2006.05.001

Zhang, R., Tang, X., You, S., Duan, K., Xiang, H., & Luo, H. (2020). A novel feature-level fusion framework using optical and SAR remote sensing images for land use/land cover (LULC) classification in cloudy mountainous area. Applied Sciences (Switzerland), 10(8), 1–24. https://doi.org/10.3390/APP10082928

Zhongming, Z., Linong, L., Xiaona, Y., Wangqiang, Z., & Wei, L. (2021). Climate change leads to 18.52% decrease in snow cover in Himachal: Study.